LETTER

Digital Halftoning through Approximate Optimization of Scale-Related Perceived Error Metric

Zifen HE[†], ***Nonmember and*** **Yinhui ZHANG**[†a)], ***Member***

SUMMARY This work presents an approximate global optimization method for image halftone by fusing multi-scale information of the tree model. We employ Gaussian mixture model and hidden Markov tree to characterized the intra-scale clustering and inter-scale persistence properties of the detailed coefficients, respectively. The model of multiscale perceived error metric and the theory of scale-related perceived error metric are used to fuse the statistical distribution of the error metric of the scale of clustering and cross-scale persistence. An Energy function is then generated. Through energy minimization via graph cuts, we gain the halftone image. In the related experiment, we demonstrate the superior performance of this new algorithm when compared with several algorithms and quantitative evaluation.

key words: *halftoning, approximate global optimization, multiscale error metric, scale-related*

1. Introduction

Digital halftoning is a technique for creating the illusion of continuous-tone output with a binary device, such as the laser engraving gravure, laser plate maker and digital printer. An image halftone algorithm aims to assign two labels (0 and 1) to each pixel of the image based on the properties of the pixel and its relationship with its neighbors. Effective digital halftoning can substantially improve the quality of rendered images at minimal cost [1]. In general, the properties of halftones can be broadly classified into three categories [2]. These include ordered dithering, error diffusion and optimization-based techniques.

Some approaches adopt a multiscale approach to produce an image halftone by handling the process at multiple spatial resolutions [3]–[5]. Wong considered a method for adjusting the error-diffusion filter concurrently with the error-diffusion process so that an error criterion is minimized. The minimization is performed using the least mean squares (LMS) algorithm in adaptive signal processing [6]. Kat. [7] proposed a method to produce multi-tones based on the multiscale error-diffusion technique. Key characteristics of this technique are the use of an image quad-tree and the quantization order of the pixels. Halftones of different resolutions can be embedded in a single full-scale halftone image which can provide the better image quality at different resolutions [8]. Fung proposed an algorithm that supports parallel processing and can further reduce the computational complexity [9]. Fung also proposed a MED algorithm to produce halftones of desirable green noise characteristics [10].

In the digital halftoning algorithms, the quantization of the binary pixels are cast into optimization of error metric function using maximum likelihood, least squares, direct binary search and geometry planning, which can get the optimal configuration of the binary pixels to a certain extent. Unfortunately, those algorithms can not achieve alternating scale of error metric model. High scale error measure information dissemination can not guide lower-scale error, which is only guaranteed to produce a local optimum. In this paper, an image halftone is converted into approximate global optimization of scale-related perceived error metric problem, which to gain the best possible configuration of the binary pixels in the image halftone.

In Sect. 2, we give a function modeling framework for multiscale perception error metric. In Sect. 3, the function of scale-related perceived error metric is established by use of Gaussian mixture and hidden Markov tree modeling. Experimental results and discussion are derived in Sect. 4. In Sect. 5, conclusions are drawn.

2. Multi-Scale Perception Error Metric Function Modeling Framework

Halftoning rests upon the fact that the eye acts as low-pass filter. The human visual system is not only sensitive to the spatial domain error metric information, but also to the same as frequency and direction domain. This paper also put them into a framework for multiscale objective function. The eye model we use is based on estimates of the spatial, frequency and direction sensitivity of the eye by Nasanen [11], which found the following filter frequency response to be good for predicting the subjective quality of the coded images.

$$H_r(f_r) = \exp\left(\frac{-f_r}{c \log L + d}\right) \tag{1}$$

Where $c = 0.525$, $d = 3.91$ and $L = 11$. Visual contrast sensitivity describes the signal processing properties of the visual system near threshold contrast. For sinusoidal gratings contrast is defined as $c = \frac{L_{\max}-L_{\min}}{L_{\max}+L_{\min}} = \frac{A}{L}$. where $L_{\max}$ and $L_{\min}$ are the maximum and minimum luminance, respectively. A is the luminance amplitude and L is the average luminance. The visual resolution frequency for periodic two-dimensional luminance wave-forms can be calculated

Manuscript received July 20, 2015.
Manuscript revised October 3, 2015.
Manuscript publicized October 20, 2015.

[†]The authors are with the Faculty of Mechanical and Electrical Engineering, Kunming University of Science and Technology, Kunming 650500, China.
a) E-mail: yinhui_z@163.com

DOI: 10.1587/transinf.2015EDL8156

by solving the fundamental frequency f from the following the equation $f_r = f[m^2+n^2]^{1/2}$, f_r is the fundamental spatial frequency of the periodic signal.

Define multiscale error metric information $e_{i,j}(m,n)$ of the wavelet domain spatial point (m,n) is the corresponding wavelet coefficients of the Euclidean distance in L $*$ a $*$ b $*$ space, where the scale $i \in \{1,2,3,4\}$, orientation $j \in \{1,2,3\}$.

Multiscale perception error metric objective function $\varepsilon_{i,j}(m,n)$ is built on the scale i, in the direction of j and spatial point (m,n).

$$\varepsilon_{i,j}(m,n) = e_{i,j}(m,n) * H_r(f_r) \tag{2}$$

The overall perception error metric Ψ is the sum of mean square in different locations, scales and orientations.

$$\Psi = \sum_{i,j}\sum_{m,n}\left|\varepsilon_{i,j}(m,n)\right|^2 \tag{3}$$

3. Multiscale Perception Error Metric Function

3.1 Discrete Wavelet Transform

The multiscale information of L*a*b* space is shown as Fig. 1. Figure 1 (b) shows the discrete wavelet transform of the original image through Harr wavelet [12], in which the two properties of wavelet coefficient distribution, intra-scale clustering and inter-scale persistence are evident. We can see that most of the energy compacted onto a few wavelet coefficients with large magnitudes while most of the wavelet coefficients are very small. This compact property allows us to capture the key characteristics of an image from a few large wavelet coefficients.

3.2 Intra-Scale Clustering and Inter-Scale Persistence Properties

We apply Gaussian mixture model and Hidden Markov tree (HMT) proposed [13] to character the intra-scale clustering and inter-scale persistence properties of the detail coefficients, respectively.

To gain intra-scale clustering distribution properties, a hidden stochastic state variable x_s is linked to each wavelet coefficient w_s. The x_s takes two values: either $x_s = 1$ or $x_s = 0$. Since most of the wavelet coefficients have small values while only a few wavelet coefficients have large values. The wavelet coefficients of the larger threshold are regarded as the Gaussian probability density function of the larger variance. Analogously, the wavelet coefficients of the smaller threshold are regarded as the Gaussian probability density function of the smaller variance. Thus the probability density function (pdf) $p(w_s)$ of each wavelet coefficient is well approximated by a two-density Gaussian mixture model.

$$p(w_s) = \sum_{i=0}^{1} p(x_s = i)p(w_s \mid x_s = i)$$

More specifically, $p(w_s \mid x_s = i)$ follows zero-mean Gaussian distribution.

$$p(w_s \mid x_s = i) = \frac{1}{\sqrt{2\pi\sigma_i^2}}\exp\left(\frac{-w_s^2}{2\sigma_i^2}\right) \tag{4}$$

where σ_i^2 is the variance at node i when the state is x_s, $x_s \in \{0,1\}$. The variance value is the size of threshold value of the wavelet coefficients. Upon the assumption that the wavelet coefficients are mutually independent, the joint probability density function of the wavelet coefficients is given by

$$p(W) = \prod_{s\in V} p(w_s) \tag{5}$$

where W is a matrix containing the detail coefficients of LH, HL and HH sub-band.

We apply the HMT model for the purpose of capturing inter-scale persistence properties in wavelet domain. The quad-tree probability graph structure of HMT model with three scales is shown as Fig. 2.

The black nodes represent the wavelet coefficients w_s and the white nodes represent each wavelet coefficient corresponding to hidden state variables x_s.

A hidden state variable corresponds to the four hidden state variables of next scale. The line represents the dependence of the wavelet coefficients of parent-children, namely inter-scale persistent. In the HMT model, we use the probability mass function $p(x_s = i) = \begin{bmatrix} p(x_s = 0) \\ p(x_s = 1) \end{bmatrix}$. The state transition probability $1_s^{p(s)}$ is defined to represent the probability for w_s to be 0 (or 1) when its parent $w_{p(s)}$ is 0 (or

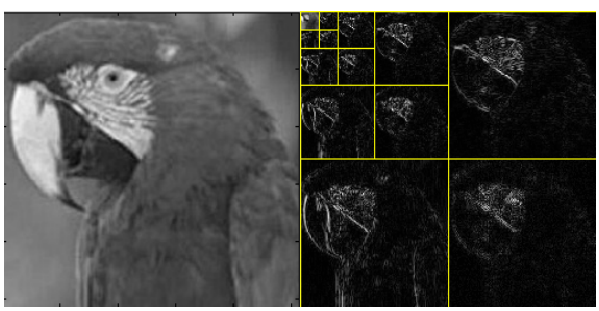

(a) (b)

Fig. 1 The original image and the DWT transform (a) original image (b) four levels DWT transform.

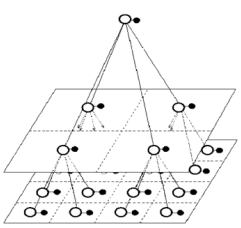

Fig. 2 The quad-tree probability graph structure.

1).

$$1_s^{p(s)} = \begin{bmatrix} 1(x_s = 0 \mid x_{p(s)} = 0)1(x_s = 0 \mid x_{p(s)} = 1) \\ 1(x_s = 1 \mid x_{p(s)} = 0)1(x_s = 1 \mid x_{p(s)} = 1) \end{bmatrix}$$

We gain the HMT model for each LH, HL and HH sub-band.

$$\Theta = \{p, \epsilon_v^u, \sigma_i^2 \mid (u, v) \in E\}$$

We employ the sub-band independence assumption and the complete HMT model is thus

$$p(W \mid \Theta) = p(W^{LH} \mid \Theta^{LH}) p(W^{HL} \mid \Theta^{HL}) p(W^{HH} \mid \Theta^{HH}) \tag{6}$$

The scale-related perceived error metric function of label i in G is given by

$$\tilde{\Psi}(x) = \lambda \tilde{\Psi}_R(x) + \tilde{\Psi}_B(x) \tag{7}$$

where $i \in \{1, 2, \ldots, c\}$, $c = 2$. $\tilde{\Psi}_R$ and $\tilde{\Psi}_B$ are represent the smoothness and singularity constrains, respectively. λ is a weight factor and equals to 1.1. The smoothness constrains is negative log-likelihood of the brightness threshold in L ∗ a ∗ b ∗ space.

$$\tilde{\Psi}_R(x_v) = -\sum \log p(L(v) \mid x_v = s) \quad \text{where} \quad s \in \{0, 1\}.$$

The singularity constrains is exponential function.

$$\tilde{\Psi}_B(x_u, x_v) = \sum_{(u,v) \in E} \exp(-(L(u) - L(v))^2 / 2\sigma_i^2) \tag{8}$$

3.3 Energy Function Minimization

A directed graph $G = (V \cup \{s, t\}, E)$ is constructed at the pixel resolution level, which expressions modeling framework. The node set of V in G contains two terminal nodes, namely, source s and sink t and E is a set of arcs. The s-t cut in G is a set of arcs whose remover partitions the nodes into two disjoint subsets S and T, such that $s \in S$ and $t \in T$ and no path can be established between s and t. Each node corresponds with the perception error measure. The minimum s-t cut is the maximum flow problem, whose classic combinatorial problems that can be solved by various of polynomial-time algorithms [14].

In this paper, we employ the min-cut method proposed in to implement energy function minimization. The energy minimization is an iterative process, which includes three stages. Firstly, the active nodes search adjacent non-saturated edges and capture new children from free nodes. The search trees expand until they fall across a neighboring node that belong to another tree. A path P from s to t is tested. Secondly, the residual graph is expanded by pushing the flow, through the path P, the amount of which is the bottleneck capacity. Once ligature on P becomes saturated, its son becomes an orphan. So, the search trees turn into forests after expanding. Lastly, every orphan strives hard to seek a new effective parent within the same as search tree in adoption stage. If it does not find an effective parent of p, it becomes a free node. The algorithm terminates when the trees are separated by saturated edges. If the fine scale pixel link to s, it equals to 0. If the fine scale pixel link to t, it equals to 1.

4. Experiments

The test image is taken of 8-bit grey scale image having the dimension 256×256 for the comparison of algorithms. All halftone images are generated and printed at a resolution of 300dpi and 24inches viewing distance. We use the proposed algorithm to obtain the halftone images. In the experiment, we compare five algorithms: proposed, I. Katsavounidis [7], Y.-H. Fung [8], J.-M. Guo [15], T. Asano [16]. Figure 3 shows the subjective results for the 'Macaw' image. The results show that this method achieves the better quality halftones that combine smooth gray tone reproduction and good edge and detail reproduction in the same image.

To further examine the performance of the proposed algorithm, we compare the proposed algorithm with the other methods. Results are presented in Table 1 for halftoning using test image Macaw.

And from the objective results it was found that the proposed algorithm achieves consistently lower values of MSEv than the other algorithms, and the value of MSEv

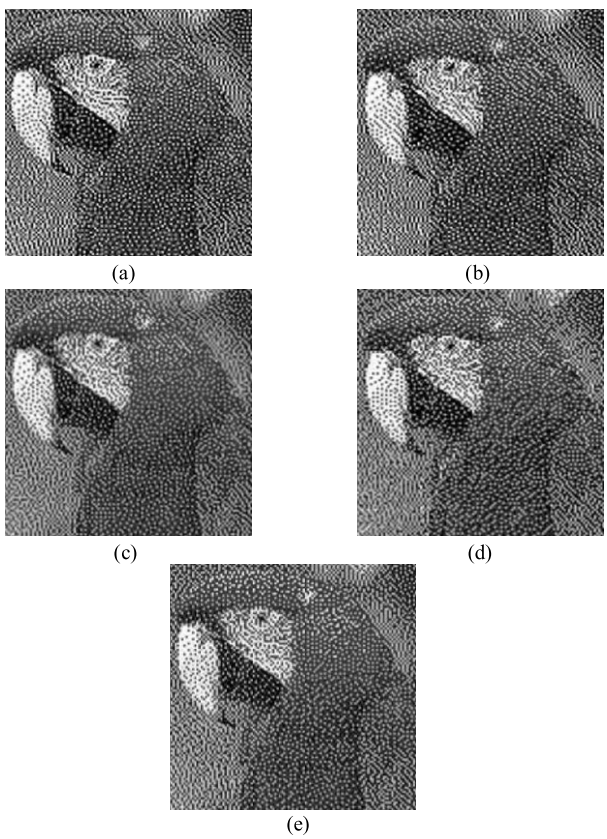

Fig. 3 Comparison of halftone image (a) [7] (b) [8] (c) [15] (d) [16] (e) proposed.

Table 1 Quality measurement of halftone image with different algorithms in terms of PSNR and MSEv.

Algorithms	Proposed	[16]	[15]	[8]	[7]
PSNR(dB)	35.7871	32.8475	31.0932	29.5537	26.9171
MSEv($\times 10^{-3}$)	0.0542	0.0863	0.1038	0.1217	0.1267

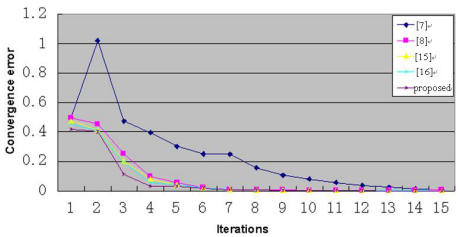

Fig. 4 Comparison of the number of iterations for the test image.

Table 2 Average elapsed time of the test image during iteration (seconds).

ζ	Proposed	[16]	[15]	[8]	[7]
10^{-1}	3.65	3.67	3.67	3.68	3.69
10^{-2}	5.44	5.62	5.65	5.78	6.05
10^{-3}	5.68	5.75	5.83	5.92	7.02
10^{-4}	6.58	6.60	6.73	6.95	7.31
10^{-5}	7.91	7.95	7.99	8.47	8.93

is also decreases. We can be seen from the Table 1 that the proposed algorithm achieves consistently higher values of PSNR than the other algorithms, and the value of PSNR are also increase. The parameter that needs to be selected is the termination condition in the iteration, which is selected as 10^{-2} during the running of the program. The result is illustrated in Fig. 4.

The convergence errors of [8], [15] and [16] dropped down to 10^{-2} just in eight iterations. The proposed algorithm is terminated with six iterations. Therefore the convergence speed of the proposed algorithm is relatively rapid.

To evaluate the computation cost, we calculate the average elapsed time of the test image when different termination conditions are selected. The test results are shown in Table 2.

The average elapsed time of the proposed algorithm increase rapidly with the decrease of ζ. We can be seen from the Table 2 that the proposed algorithm achieves consistently lower values of the time than the other algorithms. Considering the computational time of proposed algorithm, these are very significant gains.

5. Conclusions

In this paper, we proposed a method for digital halftoning through approximate global optimization of scale-related perceived error metric, which is a new halftone technique employed in printing systems. Research on the methods of multiscale modeling via 2D discrete wavelet transform, on this basis, the inter-scale modeling and intra-scale communication method of the multiscale image model are built. The energy term is generated, which consists of boundary and regional term. We applied an energy minimization method using graph cut to calculate the minimum cut of the arc weighted directed graph constructed at the pixel resolution level. We identified the "Macaw" image and tested the MSE_V and PSNR of the proposed method. Quantitative evaluation of the algorithm shows that our method is superior to other methods in the iterations speed and lower computation time.

Acknowledgments

This work was supported by the National Science Foundation of China (NSFC) under Grants 61302173 and 61461022 and Foundation of Kunming University of Science and Technology under Grant 14118777.

References

[1] C.A. Bouman, Digital Halftoning, Digital Image Processing, Jan. 2010.
[2] J.P. Allebach, ed., Selected Papers on Digital Halftoning, vol.MS 154, SPIE:Bellingham, WA, 1999.
[3] G. Sarailidis and I. Katsavounidis, "A multiscale error diffusion technique for digital multitoning," IEEE Trans. Image Process., vol.21, no.5, pp.2693–2705, 2012.
[4] Y.-H. Chan, "A modified multiscale error diffusion technique for digital halftoning," IEEE Signal Process. Lett., vol.5, no.11, pp.277–280, 1998.
[5] Y.-H. Chan and S.M. Cheung, "Feature-preserving multiscale error-diffusion for digital halftoning," J. Electron. Imaging, vol.13, no.3, pp.639–645, 2004.
[6] P.W. Wong, "Adaptive error diffusion and its application in multiresolution rendering," IEEE Trans. Image Process., vol.5, no.7, pp.1184–1196, 1996.
[7] I. Katsavounidis and C.-C.J. Kuo, "A multiscale error diffusion technique for digital halftoning," IEEE Trans. Image Process., vol.6, no.3, pp.483–490, 1997.
[8] Y.-H. Fung and Y.-H. Chan, "Embedding halftones of different resolutions in a full-scale halftone," IEEE Signal Process. Lett., vol.13, no.3, pp.153–156, 2006.
[9] Y.-H. Fung, K.-C. Lui, and Y.-H. Chan, "Low-complexity high-performance multiscale error diffusion technique for digital halftoning," J. Electronic Imaging, vol.16, no.1, pp.35–44, 2007.
[10] Y.-H. Fung and Y.-H. Chan, "Green noise digital halftoning with multiscale error diffusion," IEEE Trans. Image Process., vol.19, no.7, pp.1808–1823, 2010.
[11] R. Nasanen, "Visibility of halftone dot textures," IEEE Trans. Syst., vol.SMC-14, no.6, pp.920–924, 1984.
[12] A. Haar, "Zur theorie der orthogonalen funktionensysteme," Math. Ann., vol.69, no.3, pp.331–371, 1910.
[13] M.S. Crouse, R.D. Nowak, and R.G. Baraniuk, "Wavelet-based statistical signal processing using hidden Markov models," IEEE Trans. Signal Process., vol.46, no.4, pp.886–902, 1998.
[14] K. Li, X. Wu, D.Z. Chen, and M. Sonka, "Optimal surface segmentation in volumetric images – A graph-theoretic approach," IEEE Trans. Pattern Anal. Mach. Intell., vol.28, no.1, pp.119–134, 2006.
[15] J.-M. Guo and Y.-F. Liu, "Improved dot diffusion by diffused matrix and class matrix co-optimization," IEEE Trans. Image Process., vol.18, no.8, pp.1804–1816, 2009.
[16] T. Asano, P. Brass, and S. Sasahara, "Disc covering problem with application to digital halftoning," Theory of Computing Systems, vol.46, no.2, pp.157–173, 2010.